Oxidation–reduction reactions of simple hydroxamic acids and plutonium(IV) ions in nitric acid

By M. J. Carrott[1], O. D. Fox[1], G. LeGurun[1], C. J. Jones[1], C. Mason[1], R. J. Taylor[1,*], F. P. L. Andrieux[2] and C. Boxall[2]

[1] British Technology Centre, Nexia Solutions, Sellafield, Seascale CA20 1PG, UK
[2] Centre for Materials Science, University of Central Lancashire, Preston PR1 2HE, UK

Summary. Simple hydroxamic acids such as formo- and aceto-hydroxamic acids have been proposed as suitable reagents for the separation of either Pu and/or Np from U in modified or single cycle Purex based solvent extraction processes designed to meet the emerging requirements of advanced fuel cycles. The stability of these hydroxamic acids is dominated by their decomposition through acid hydrolysis. Kinetic studies of the acid hydrolysis of formo- and aceto-hydroxamic acids are reported in the absence and the presence of Pu(IV) ions. The slow reduction of these plutonium(IV) hydroxamate complexes to Pu(III) aquo-ions has been characterised by spectrophotometry and cyclic voltammetry. The reductions of Pu(IV) in the presence of FHA and AHA are consistent with a mechanism in which free hydroxamic acid in solution is hydrolysed whilst Pu(IV) ions remain fully complexed to hydroxamate ligands; then at some point close to a 1 : 1 Pu(IV) : XHA ratio, some free Pu^{4+} is released from the complex and reduction is initiated. Electrochemical and kinetic data suggest that the reductant is the hydroxamic acid rather than the hydroxylamine.

1. Introduction

Hydroxamic acids (XHA) are a particularly interesting class of organic ligands. They are O,O donor ligands of general structure [RCONHOR′], and as such can be considered as hard Lewis bases capable of interacting strongly with a range of metal ions [*e.g.* see 1–5]. As well as their complexing properties, hydroxamic acids are hydroxylamine derivatives and are easily oxidized by metal ions such as Np(VI) [6, 7]. Consequently, applications of simple hydrophilic hydroxamic ligands (R = H or CH₃) for the stripping of actinides in much simplified Purex solvent extraction flowsheets for advanced fuel cycles have been reported [8–11].

This paper describes aspects of the redox chemistry of formo- and aceto-hydroxamic acids (FHA, AHA) in the presence of Pu(IV) ions. The influences of these hydroxamic acids on the solvent extraction chemistry of Pu(IV) ions are to be reported in a companion paper [12].

2. Experimental methods

2.1 Chemicals

A Pu(III) stock solution was generated electrochemically from the stable Pu(IV) stock solution in nitric acid and the purities of Pu stock solutions were checked spectrophotometrically before use (Pu stock solutions used Magnox-derived plutonium nitrate solutions). Uranyl nitrate solution was prepared from the crystals and hydroxylamine nitrate by the addition of stoichiometric amounts of AgNO₃ to hydroxylamine chloride. Fe(III) was prepared from crystals of Fe(NO₃)₃·9H₂O (Sigma-Aldrich). Analytical grade reagents were used where available. FHA (custom synthesis, Tocris Cookson) and AHA (Sigma-Aldrich) solutions were prepared from the solids, the purity of synthesised FHA was verified from ¹H-NMR in combination with analytical data. FHA and AHA crystals were stored in a refrigerator to minimise decomposition and all solutions were made up in distilled or deionised water when required.

2.2 XHA hydrolysis

The hydrolysis kinetics for FHA and AHA were measured using a colorimetric method [13, 14]. HNO₃ and XHA solutions were equilibrated at specific temperatures in a water bath prior to mixing. At intervals, small samples were taken and diluted in to excess Fe(III) solution (0.01 M HNO₃). This simultaneously forms the Fe(III)-XHA complex and quenches the hydrolysis. The absorption spectrum of the red coloured complexes formed were then recorded and used to determine XHA concentration from a previously established calibration curve. The Fe(III)-FHA complex analysed showed a broad peak centred at ∼ 489 nm whilst the Fe(III)-AHA complex had a peak maxima ∼ 499 nm. Note that it was important to sample the XHA-HNO₃ solutions and to add the Fe(III) reagent separately to each sample, as we have shown elsewhere that the Fe(III)-XHA complex itself hydrolyses at a different rate than free XHA [15]. Standard kinetic methods were used to analyse the data [16].

*Author for correspondence
(E-mail: robin.j.taylor@nexiasolutions.com).

2.3 Plutonium(IV) – XHA reduction experiments

Standard well established methods in plutonium chemistry and chemical kinetics were used throughout this part of our studies. Stock solutions were mixed in an optical cuvette and equilibrated at the desired temperature. (*N.b.* a last set of 5 experiments were performed at a later date using a Zeiss UV/Vis spectrometer coupled *via* fibre optics to a dipping optrode for direct measurement of a reaction solution of 25 mL volume in a glovebox). The reducing agent (hydroxylamine nitrate (HAN), XHA) was added last, the solutions mixed and the absorption spectra recorded over time. A water jacket connected to a thermostatically controlled water bath was used to maintain specific reaction temperatures in the cuvette. The reduction reaction was followed over time using the growth of the Pu(III) absorption band at ~ 905 nm [17], because the intense Pu(IV)-XHA absorption peaks [18, 19] vary slightly depending on the actual speciation. The procedures were checked initially by validation against the well known Pu(IV)-HAN reaction [20].

Certain difficulties encountered in these studies should be noted. In particular, obtaining reproducible and self-consistent sets of experimental data did not prove to be straightforward. Particularly, in some early experiments reduction appeared to occur rather rapidly with FHA, often with no induction period. This was ascribed to two potential problems in the procedures, (a) the use of 'aged' XHA crystals which may have deteriorated during storage and (b) the use of heating to accelerate dissolution of XHA in concentrated stock solutions. These early experiments were therefore disregarded and (a) new batches of FHA and AHA were obtained and (b) less concentrated stock solutions were prepared under mild ambient conditions only. Interestingly, these failed experiments, however, do indicate the sensitivity of the system to XHA decomposition (hydrolysis), which will be discussed in detail in Sects. 3.1 and 3.2.

Ultimately, 78 useful kinetic experiments were performed; these can be described in categories according to the experimental parameters under investigation:

1. AHA experiments at ambient temperatures (~ 20 or 25 °C) with (i) variable AHA and (ii) variable HNO_3 concentrations.
2. AHA experiments at elevated temperatures (40 °C) with (i) variable HNO_3, (ii) increasing ionic strength (added $NaNO_3$), (iii) added U(VI) ions and (iv) varying initial [Pu].
3. AHA experiments in 1 M HNO_3 at varying temperatures (30–70 °C).
4. AHA experiments with variable initial concentrations of Pu(III) (40 °C).
5. FHA experiments at 20 °C with (i) variable HNO_3, (ii) increasing ionic strength (added $NaNO_3$), (iii) added U(VI) ions, (iv) varying initial [Pu], (v) varying FHA.
6. FHA experiments at an elevated temperature (50 °C) and constant [HNO_3] with varying FHA.
7. FHA experiments in 1 M HNO_3 at varying temperatures (5–65 °C).
8. FHA experiments with HAN initially present in the reacting solution (40 °C).
9. A series of 4 FHA experiments in which the FHA concentration was followed using the colorimetric sampling

method described previously rather than the Pu(III) absorbance (experimental conditions as in Fig. 5).

2.4 Electrochemistry

Three stock solutions were prepared containing 5 M HNO_3, 0.1 M AHA and 0.01 M Pu(IV), respectively. These were then used to prepare 25 mL aliquots of solutions containing Pu(IV) for the electrochemical studies. Each of these solutions contained 0.001 M Pu(IV) but had varying acidity and AHA : Pu ratios between $1 : 2$–$20 : 1$ ([AHA] = 0.0005–0.02 M; [HNO_3] = 0.1–3.5 M). A Pu only sample at 0.1 M HNO_3 was also prepared.

Compared to the *ca.* 1 g/L concentrations more typical of Purex process solutions, 0.001 M Pu(IV) (0.24 g/L) solutions were used for the electrochemical measurements to give lower current densities. The electrochemistry of the solutions was investigated by cyclic voltammetry (CV) using an EG&G Princeton Applied Research (PAR) Potentiostat/Galvanostat model 263A and a PAR three electrode cell incorporating an Ag/AgCl reference electrode (SSCE) and a Pt auxilliary electrode. Vitreous carbon and Pt disc working electrodes were used for the measurements although the carbon electrode generally showed less well defined waves than the Pt electrode. However, on carbon the accessible potential range extended to -0.8 V *vs.* SSCE whereas on Pt reductive solvent breakdown occurred at -0.2 V *vs.* SSCE. The electrochemical cell was fitted with an argon supply to allow solutions to be purged with Ar and maintained under an Ar atmosphere while measurements were made. Aliquots of $K_3[Fe(CN)_6]$ solution were added at the end of the measurements to provide an internal reference, noting that the potential of the $[Fe(CN)_6]^{3-/4-}$ couple is dependent on the nature of the supporting electrolyte, including its ionic strength and pH [21].

The waves in the cyclic voltammograms were described by:

i) the peak anodic and cathodic currents measured by the potentiostat with respect to the horizontal potential/*x*-axis, i_{pa} and i_{pc} respectively,
ii) the peak anodic and cathodic currents within the cyclic voltammogram *i.e.* the height of the peaks above their prevailing background currents, i_{da} and i_{dc} respectively; and
iii) the corresponding peak potentials E_{pa} and E_{pc} respectively.

No compensation for internal cell resistance, R, was applied during the measurement but plots of ($E_{pa} - E_{pc}$), ΔE_p, against ($i_{pa} - i_{pc}$), Δi_p, or plots of E_{pa} against i_{pa} were used to estimate R so that a correction for iR drop could be applied where necessary. Although the values of the peak potentials can be significantly affected by uncompensated cell resistance, the formal electrode potential, E_f given by ($E_{pa} + E_{pc}$)/2 for reversible/Nernstian systems, is usually much less sensitive. In the examples studied here uncompensated cell resistance might typically result in an overestimate of E_f by between 1 and 5 mV. To monitor Pu oxidation state, electronic absorption spectra (EAS) of the solutions were measured over the wavelength range 350–900 nm using a Perkin

Elmer Lambda 900 spectrophotometer connected *via* fibre optics to the glovebox.

3. Results and discussion

3.1 XHA hydrolysis

Hydroxamic acid hydrolysis produces hydroxylamine and the parent carboxylic acid. It is an acid catalysed reaction and in acid solutions the hydroxylamine formed becomes protonated (Eq. (1)) [22]. This instability is a key feature of XHA chemistry that must be accounted for in any process flowsheet design [9]. Conversely, it is actually beneficial in the downstream decomposition of the ligand after separation. It is also fundamental in understanding XHA redox and complexation chemistry.

$$RCONHOH + H_2O + H^+ \rightarrow RCOOH + NH_3OH^+ \qquad (1)$$
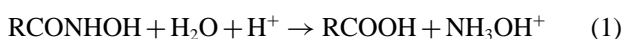
Miles and Temple [13] had previously shown that FHA hydrolysis was a 2nd order reaction overall, 1st order with respect to both FHA and HNO_3. Our data confirmed this, with all experiments for both FHA and AHA conforming to Eq. (2), where $a_0 = [FHA]_0$, $b_0 = [HNO_3]$ and $x = [FHA]_0 - [FHA]_t$ [16]. Results are given in Tables 1–2 for both FHA and AHA.

$$\frac{1}{a_0 - b_0} \ln\left(\frac{b_0(a_0 - x)}{a_0(b_0 - x)}\right) = kt \qquad (2)$$

The hydrolysis equation (Eq. (3)) was, therefore, determined for both FHA and AHA where rate constants at 25.0 °C are $0.016 \pm 0.001\,\mathrm{dm^3\,mol^{-1}\,min^{-1}}$ for FHA and $0.00205\,\mathrm{dm^3\,mol^{-1}\,min^{-1}}$ for AHA and activation energies were found to be $77.3 \pm 1.6\,\mathrm{kJ\,mol^{-1}}$ (FHA) and $79.9 \pm 2.9\,\mathrm{kJ\,mol^{-1}}$ (AHA) [19].[1] The value for AHA is close to that reported by Mane and Jagdale in HCl [24] ($82.4\,\mathrm{kJ\,mol^{-1}}$). Note that this equation is only valid up to 3 M HNO_3 as it is well known that at higher acidities a maximum rate is reached. For a more detailed review of the kinetics and mechanisms of the acid catalysed hydrolysis of hydroxamic acids, the interested reader is referred to Ref. [22] and references therein.

$$-\frac{d[XHA]}{dt} = k[XHA][H^+] \qquad (3)$$

Little variation in the rate constants for AHA or FHA hydrolysis was found on introducing either nitrate (as $NaNO_3$) or uranyl nitrate in to the solution (Table 2), although the nitrate data for FHA showed a weak dependency ($\propto [NO_3^-]^{-0.2}$). This appears to be consistent with previous studies that showed a positive ionic strength effect. See, for instance, the data of Mane and Jagdale [23, 24] where AHA and hexanohydroxamic acid hydrolysis rates at constant acidity show a chloride dependency of

---

[1] More accurately, the order with respect to acidity in the AHA case was actually 0.9. This is consistent with apparent orders with respect to [H+] calculated from the data of Mane and Jagdale between 0–3.0 M acid concentrations for: hexanohydroxamic acid [23] in HCl and H_2SO_4, isobutyrohydroxamic acid in HCl and H_2SO_4 [14] and aceto-, isobutyl- and hexyl- hydroxamic acids in H_2SO_4 [24].

Table 1. Kinetic analyses of free AHA and FHA hydrolysis rates ([XHA] = 0.05 M).

	Acidity (M)	Temperature (°C)	Rate constant (min^{-1})
AHA	0.5	50	0.0157
AHA	1	50	0.0245
AHA	1.5	50	0.0334
AHA	2	50	0.06
AHA	2	50	0.0516
AHA	3	50	0.0391
AHA	3	50	0.0721
AHA	3	50	0.0735
AHA	1	58	0.04807
AHA	1	56.2	0.03689
AHA	1	50.2	0.02541
AHA	1	46.8	0.01885
AHA	1	41.2	0.00977
AHA	1	37.6	0.00615
AHA	1	34.7	0.00435
AHA	1	31	0.00411
AHA	1	28.4	0.00243
AHA	1	25	0.00211
FHA	1	25	0.000267[a]
FHA	1	25.3	0.00025
FHA	1	30.4	0.00042
FHA	1	35.3	0.00075
FHA	1	40.2	0.00115
FHA	1	45	0.00186
FHA	1	49.7	0.00316
FHA	1	55.6	0.00455
FHA	1	59.6	0.00605

a: Miles and Temple [13].

ca. 0.1–0.2. Even less variation on the rate with added nitrate ions was observed in the AHA case. For all cases between 1 and 7 M total nitrate the observed AHA hydrolysis closely followed the calculated curves for Eq. (3) with the pseudo-1st order rate constant only increasing from 1.67×10^{-5} to $1.73 \times 10^{-5}\,\mathrm{dm^3\,mol^{-1}\,s^{-1}}$ across this range at 20 °C (Table 2). These findings differ from the conclusions drawn by Karraker [25], who observed a substantially decreased AHA half-life on introducing both $NaNO_3$ and uranyl nitrate.

3.2 Plutonium(IV) reduction by simple hydroxamic acids

3.2.1 Experimental results

It has previously been observed that in the presence of aceto- and formo-hydroxamic acids in nitric acid, dark red Pu(IV)-hydroxamate complexes are gradually reduced to blue Pu(III) aquo-ions, with the corresponding changes in the absorption spectra confirming such reduction [19]. In order to more fully understand the hydroxamate chemistry of Pu and to design robust separation process flowsheets, we needed to better understand these reactions. It should be noted that the data gathered during this exercise was mainly under conditions relevant to the broad envelope of flowsheet operations rather than being ideally suited to kinetic analysis. This has complicated subsequent data interpretation, particularly at high [XHA]. At the high XHA (particularly FHA) concentrations used in some of these experiments, we note that it seems likely that activity effects will become

Table 2. Comparison of experimentally determined and calculated rate constants for FHA and AHA hydrolysis with variable total nitrate and uranyl nitrate concentrations.
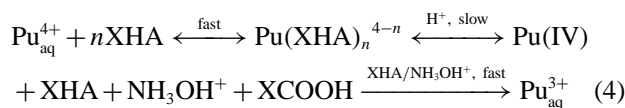
$[XHA]_0$ (M)	X	$[NO_3^-]$ (M)	$[U(VI)]$ (M)	$[H^+]$ (M)	T (°C)	$k_{(calc)}$ (dm^3 mol^{-1} s^{-1})	$k_{(expt)}$ (dm^3 mol^{-1} s^{-1})
0.04	F	1.6	0	0.8	40	0.00113	0.00106
0.0333	F	2	0	0.67	40.3	0.00117	0.00122
0.0286	F	2.86	0	1.14	40	0.00113	0.00117
0.0125	F	3.5	0	1	40	0.00113	0.00134
0.0333	F	1.00	0.165	0.67	24	0.00023	0.00018
0.0242	F	2.27	0.126	2.02	21.1	0.00017	0.00019
0.0395	F	1.81	0.099	1.61	21.1	0.00017	0.00018
0.00512	A	1.00	0	1.00	20	1.84×10^{-5}	1.67×10^{-5}
0.00487	A	1.99	0	1.00	20	1.84×10^{-5}	1.66×10^{-5}
0.00490	A	3.00	0	1.00	20	1.84×10^{-5}	1.67×10^{-5}
0.00487	A	4.00	0	1.00	20	1.84×10^{-5}	1.68×10^{-5}
0.00485	A	5.04	0	1.00	20	1.84×10^{-5}	1.72×10^{-5}
0.00502	A	6.00	0	1.00	20	1.84×10^{-5}	1.70×10^{-5}
0.00485	A	6.99	0	1.00	20	1.84×10^{-5}	1.73×10^{-5}
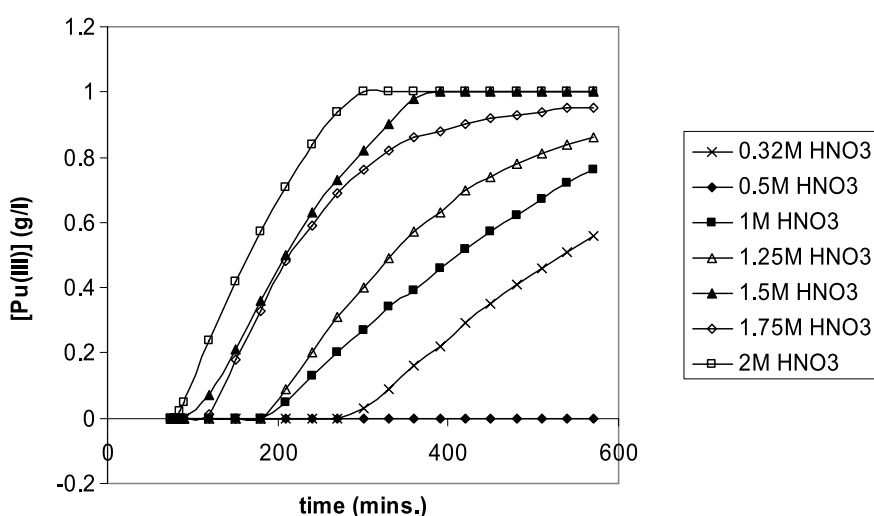
Fig. 1. Growth of Pu(III) from the reduction of Pu(IV) (1 g/L; $T = 20$ °C) by 1 M FHA in 0.5–2 M HNO$_3$. Also shown is an additional experiment at 0.32 M HNO$_3$ with 0.3 M FHA, *i.e.* [FHA] ≤ [HNO$_3$].

increasingly important, causing deviations from simple behaviours expected on a concentration basis.

The reduction is characterised by a variable induction period followed by an apparent near zero-order growth in Pu(III) concentration, measured from the Pu(III) absorption peak at ~ 908 nm (example data for FHA at varying nitric acid concentrations is shown in Fig. 1). The length of this induction period is reduced with increases in acidity or temperature and decreases in FHA concentration. The addition of uranyl or nitrate (NaNO$_3$) ions had little discernible effect on the induction periods in the FHA system but induction periods did appear to decrease in the AHA system. Interestingly, in the experiment (coded "P3X41") where initially the concentration of FHA exceeded the nitric acid concentration ([HNO$_3$] = 0.5 M; [Pu(IV)]$_0$ = 1 g/L; [FHA] = 1 M; $T = 20$ °C; filled diamond data points in Fig. 1), no reaction was observed over the duration of monitoring (> 570 min). This is not a simple acidity effect as in another experiment at 0.32 M HNO$_3$ reduction was observed. It appears to be related to the [FHA] : [HNO$_3$] ratio. The induction period in these reduction reactions is most certainly related to the hydrolysis of the hydroxamic acid. As the excess (free, unbound) hydroxamic acid in the bulk solution is hydrolysed to hydroxylamine and the carboxylic acid (*via* Eq. (1)),

the Pu(IV) speciation changes and, when some threshold is passed, de-complexed Pu(IV) becomes available for reduction (Eq. (4)). This was supported by later experiments (P5X1-4), where the ratios of Pu(IV) and AHA concentrations were varied between 3.5 : 1–1 : 2, and which showed very low inductions periods of a few minutes only.

$$\mathrm{Pu}_{aq}^{4+} + n\mathrm{XHA} \xrightleftharpoons{\text{fast}} \mathrm{Pu(XHA)}_n^{4-n} \xrightleftharpoons[\text{H}^+,\ \text{slow}]{} \mathrm{Pu(IV)}$$
$$+ \mathrm{XHA} + \mathrm{NH_3OH^+} + \mathrm{XCOOH} \xrightarrow{\text{XHA/NH}_3\text{OH}^+,\ \text{fast}} \mathrm{Pu}_{aq}^{3+} \quad (4)$$

Other qualitative comparisons can be made between the FHA and AHA data. Pu(IV) reduction is broadly similar for both cases as might be expected (Fig. 2), although the AHA reaction is markedly slower probably reflecting the greater stability of AHA compared with FHA towards hydrolysis. In some cases (at 40 °C) the reduction appeared to stop before completion with even some re-oxidation of Pu(III) back to Pu(IV) (*e.g.* Fig. 2 curve P3X23). Similarly, in experiments where [AHA] < [Pu(IV)] re-oxidation of Pu(III) back to Pu(IV) occurs (see Fig. 3). Whilst we were unable to directly measure any absorbance due to HNO$_2$ due to the Pu(IV)-AHA bands below 500 nm, it is well known that Pu(III) oxidation in nitric acid is autocatalysed by nitrous
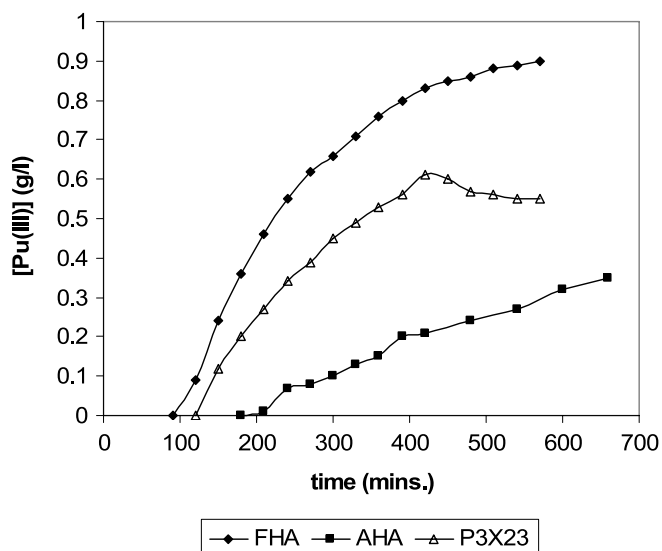
Fig. 2. Comparison of 0.1 M AHA and FHA reductions of 1 g/L Pu(IV) in 1 M HNO$_3$ ($T = 20$ °C). Also shown is experiment P3X23 where some re-oxidation of Pu(III) is observed at long times ([Pu] = 1 g/L; [HNO$_3$] = 2 M; [AHA] = 0.1 M; $T = 40$ °C).

acid that accumulates in the solution as a product of the reaction. Pu(III) can only be stabilised in HNO$_3$ by interrupting this cycle of reactions using a reagent, such as hydrazine, that reacts rapidly with nitrous acid [26]. Hydroxylamine

and hydroxamic acids also 'scavenge' nitrous acid in this fashion so presumably visible Pu(III) re-oxidation only occurs at the point at which both AHA and hydroxylamine are removed from the solution and are no longer available to scavenge nitrous acid (Fig. 3). Temperature had a major effect on reduction of Pu(IV) by both FHA and AHA as illustrated in Fig. 4 which shows the FHA-Pu(IV) data between 5 and 30 °C. At higher temperatures the reaction is completed at even quicker timescales, with the induction period completely disappearing around 50 °C (data not shown). This is most probably a combination of effects due to the increased rates of XHA hydrolysis and Pu(IV) reduction at higher temperatures and the increased generation of HNO$_2$. Clearly, further specific experiments are needed to clarify the role that HNO$_2$ has, in particular at elevated temperatures and on the later stages of the reaction.

Fig. 5 illustrates experiments P4X19–22 in which the FHA concentration rather than the Pu(III) was followed (by sampling and using the off-line colorimetric method). It is clear that the decreases in FHA concentrations in the two experiments, in the absence and presence of Pu(IV) with 1 M FHA in 1 M HNO$_3$, are essentially the same, *i.e.* the presence of 1 g/L Pu(IV) has no effect on bulk (free) FHA loss through acid hydrolysis. Also, when FHA is in excess of the HNO$_3$ (*i.e.* 1 M FHA; 0.5 M HNO$_3$) in run P4X21, the FHA hydrolysis reaches a steady state with 0.5 M FHA
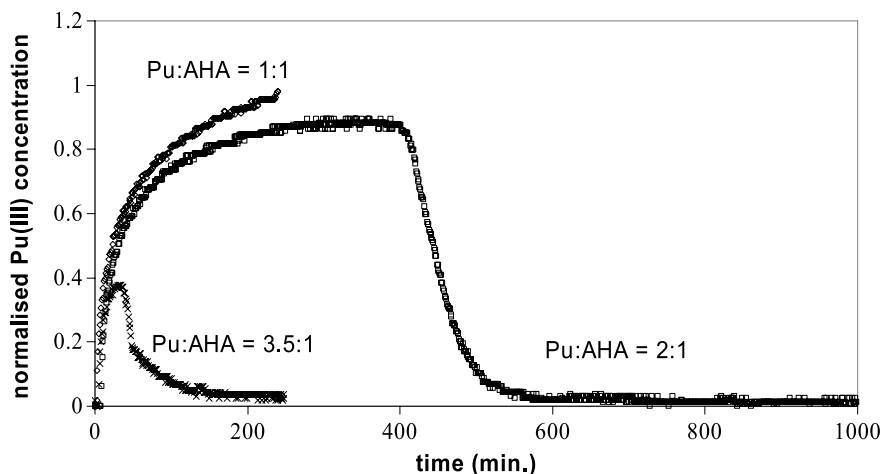

Fig. 3. Pu(IV)-AHA reduction at low molar AHA : Pu ratios ([Pu] = 1 g/L; [HNO$_3$] = 1 M; [AHA] = 0.0042–0.001 M; $T = 25$ °C).
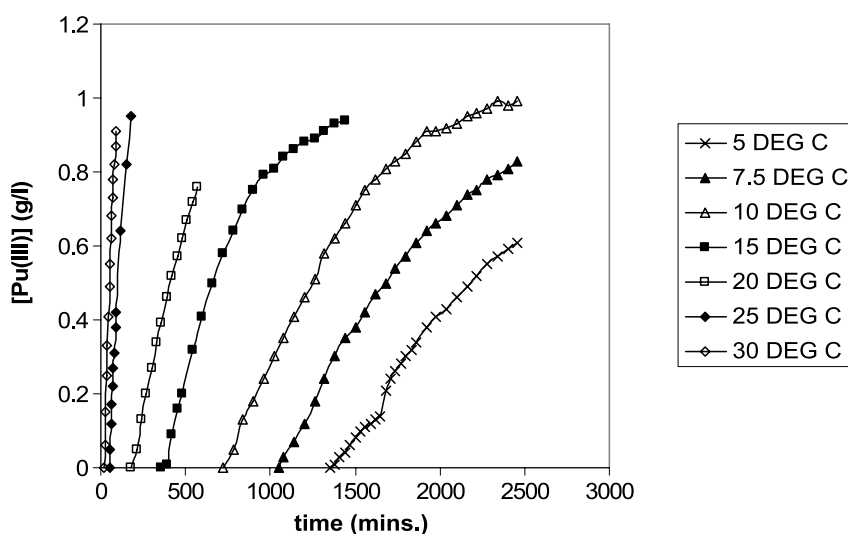
Fig. 4. Temperature dependence (5–30 °C) of the Pu(IV)-FHA reaction ([Pu] = 1 g/L; [FHA] = 1 M; [HNO$_3$] = 1 M).
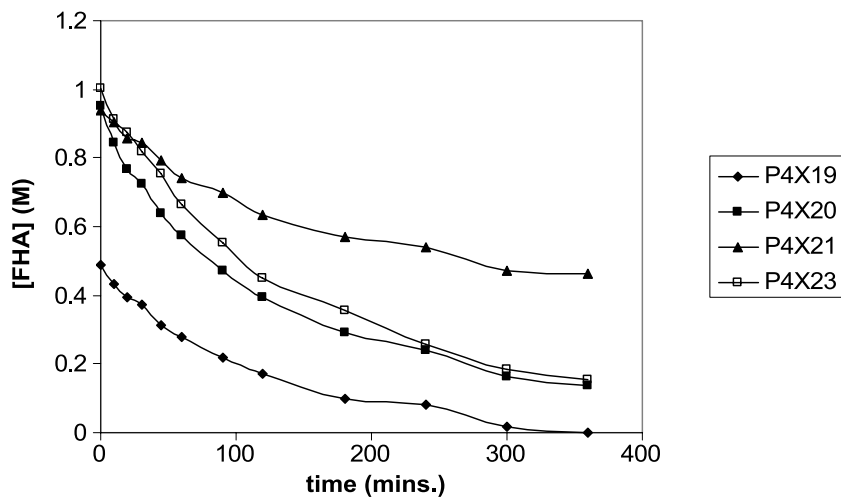
Fig. 5. The hydrolysis of FHA in HNO_3 at $20\,°C$. Where: P4X19, $[Pu(IV)] = 0\,g/L$; $[HNO_3] = 1\,M$; $[FHA] = 0.5\,M$. P4X20, $[Pu(IV)] = 0\,g/L$; $[HNO_3] = 1\,M$; $[FHA] = 1\,M$. P4X21, $[Pu(IV)] = 1\,g/L$; $[HNO_3] = 0.5\,M$; $[FHA] = 1\,M$. P4X23, $[Pu(IV)] = 1\,g/L$; $[HNO_3] = 1\,M$; $[FHA] = 1\,M$.

remaining. This is presumably due to protonation of the hydroxylamine product causing a depletion of free acidity in the solution to the point where the FHA acid catalysed hydrolysis slows to negligible levels (*i.e.* see Eq. (1)). In the reverse situation where $[HNO_3] : [FHA] = 2 : 1$, the hydrolysis proceeds normally to completion (P4X19). Finally, the similarity of all the FHA hydrolysis rate constants for experiments P4X19–21,23 suggests a reasonable self-consistency is attained in these experiments, although the actual mean value of $2.14 \times 10^{-4}\ dm^3\ mol^{-1}\ s^{-1}$ is somewhat higher than the value calculated using the accepted kinetics, see Sect. 3.1 ($1.51 \times 10^{-4}\ dm^3\ mol^{-1}\ s^{-1}$). These observations explain the lack of Pu(IV) reduction observed in P3X41 when $[XHA] > [HNO_3]$, as the 'switching off' of the hydrolysis reaction means sufficient XHA always remains in solution to complex the Pu(IV) and the threshold at which de-complexed Pu(IV) becomes available for reduction is not reached.

The addition of up to 1 M hydroxylamine nitrate (HAN) solutions to the initial reaction mixture had little discernible effects (Fig. 6); this appears to agree with an observation made by Karraker [25]. It should be noted that Barney's

Pu(IV)-HAN kinetics [20] could not be fitted to these runs with HAN added. So these experiments with HAN added to the Pu(IV)-AHA system appeared to suggest that not only is HAN probably not the reductant for Pu(IV) in this system but also in the presence of XHA it is actually prevented from reducing Pu(IV). It should be noted however that the HAN : Pu(IV) ratios probably present in this system at the end of the induction period are much higher than those studied by Barney [20].

One other interesting observation made by Karraker [25] was that AHA added to Pu(III) causes formation of the Pu(IV)-AHA complex, but this apparent oxidising ability of AHA is difficult to rationalise. We, therefore, spectroscopically followed three different solutions with initial Pu(III) concentrations of 0.2, 0.5, 1.0 g/L (no Pu(IV) present) at an AHA concentration of 0.1 M ($[HNO_3] = 1\,M$; $T = 25\,°C$). No reaction was observed with Pu(III) being stable for time periods of over 200 min. Similar experiments in the presence of 1 g/L Pu(IV) were difficult to analyse due to spectral interferences but again there was little real evidence for any oxidation of Pu(III). Fig. 3 shows Pu(III) re-oxidation can occur once the AHA and HAN are fully oxidized and no longer available in solution to scavenge HNO_2.
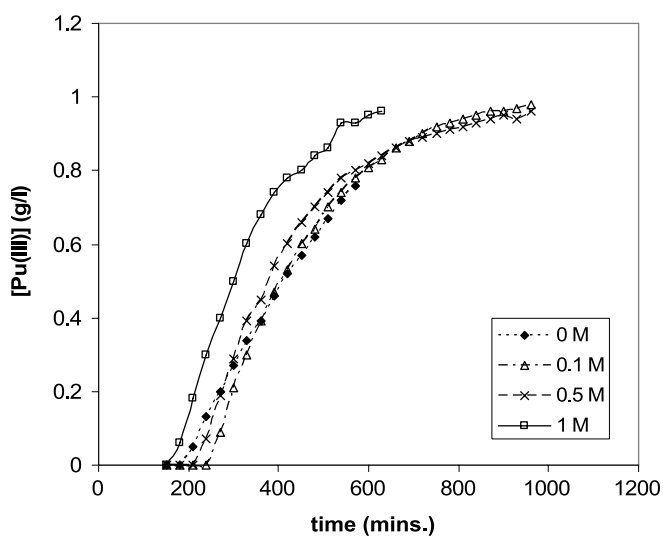

Fig. 6. Effect of adding 0–1 M hydroxylamine nitrate to the Pu(IV)-FHA reaction ($[Pu] = 1\,g/L$; $[HNO_3] = 1\,M$; $[FHA] = 1\,M$; $T = 20\,°C$).
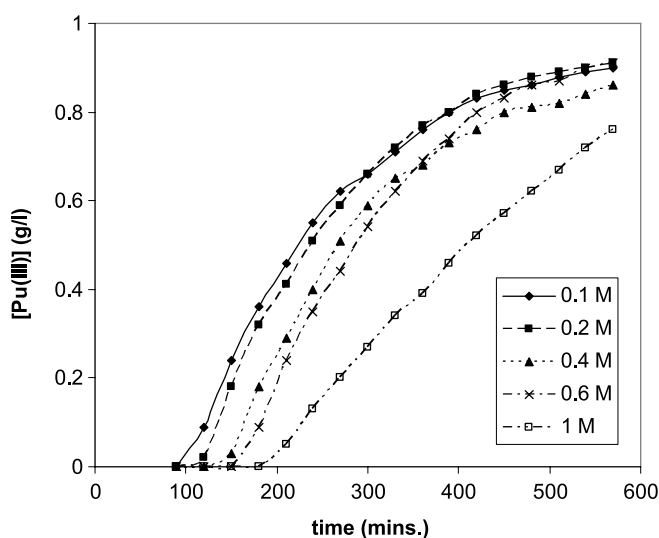

Fig. 7. Effect of variable FHA concentration (0.1–1.0 M) on the reduction of 1 g/L Pu(IV) by FHA at $20\,°C$ ($[HNO_3] = 1\,M$).
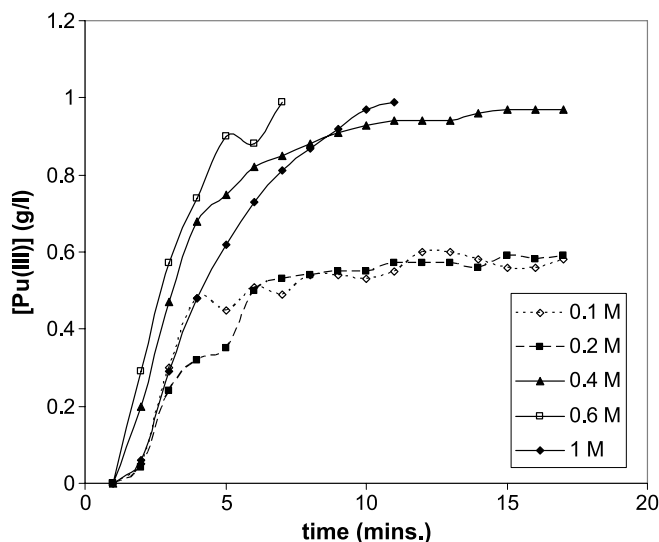
Fig. 8. Effect of variable FHA concentration (0.1–1.0 M) on the reduction of 1 g/L Pu(IV) by FHA at 50 °C ([HNO$_3$] = 1 M).

Whilst most of the experimental runs showed a near linear growth in Pu(III) which could be interpreted as apparent zero-order kinetics, some experiments at longer timescales and at low FHA concentrations showed clear deviations from this trend. Fig. 7 illustrates the experiments at variable FHA concentrations showing such changes in the Pu(III) growth curves between 0.6 and 1 M FHA. The effects of elevated temperatures on the reduction, described previously, are further illustrated by the set of experiments with variable FHA concentration at 50 °C (Fig. 8). It is also seen from this figure that at low [FHA] the reduction appears to reach a steady state around 60% completion, presumably in these runs the reductant(s) quickly became exhausted either through hydrolysis and/or reaction with HNO$_2$ generated *in situ*. Accordingly, it does seem clear from these data that the rate and extent of Pu(IV) reduction in the presence of XHA is not amenable to simple kinetic treatments (*i.e.* zero, 1st or 2nd order kinetics).

3.2.2 Discussion

The potential complexity of this system which can involve hydrolysis of free and bound XHA, up to 4 Pu(IV)-AHA complexes, two reducing agents for Pu(IV) (XHA and HAN) and other ligands (XCOOH, NO$_3^-$) has been discussed previously [27]. A preliminary analysis of the reaction rates presented therein showed that ln – ln plots of the apparent zero order rate constants, determined from the kinetic runs, against [H$^+$] at the end of the induction period and against [Pu(IV)]$_0$ gave linear plots of gradients $\sim +1.2$ and $\sim +0.8$ respectively, *i.e.* approximately unity. It was noted that the relationship between reaction rate and FHA concentration was difficult to interpret and that U(VI) and nitrate ions had little discernible effect on the reaction rates. An Arrhenius plot gave a reasonably linear relationship between ln k_{obs} and $1/T$, indicating an activation energy of ~ 90 kJ mol^{-1} and a pre-exponential factor of $\sim 2.3 \times 10^9$ s^{-1}. Taylor *et al.* [27] then calculated reaction half-lives and rate constants for FHA hydrolysis and compared these with experimental values for each kinetic

experiment, showing reasonable concordance between hydrolytic and experimental values. It was proposed that this analysis, which was admittedly of a very basic and empirical nature, indicated that the reduction of Pu(IV) in the presence of a hydroxamic acid was controlled by the rate of hydrolysis of the free hydroxamic acid. This was based on the similarity of the activation energy and pre-exponential factor, reaction half-lives and orders of reaction with respect to HNO$_3$ and initial Pu.

Qualitatively, the experimental data presented here is consistent with a situation in which Pu(IV) is strongly stabilised as the hydroxamate complex. Excess free hydroxamic acid in the bulk solution is being continually depleted through acid hydrolysis. At some critical point the complex starts to dissociate, releasing a reducible form of Pu(IV) (most probably the free Pu^{4+} (PuNO$_3^{3+}$) ion). This is represented experimentally by the end of the induction period and the appearance of Pu(III) in solution as the 'free' Pu(IV) is rapidly reduced either by the hydroxylamine formed from XHA hydrolysis or the hydroxamic acid itself. A full kinetic analysis of the AHA data has now been completed and will be reported separately [28] but it is sufficient to note here that the detailed treatment is generally consistent with the overall scheme described herein.

3.3 Pu(IV)/Pu(III) redox potential shifts due to AHA complexation

3.3.1 Cyclic voltammetry

The previous section described the reduction of Pu(IV) ions by AHA and FHA. However, the nature of the actual reductant is uncertain in that whilst hydroxamic acids are reducing agents, their hydrolysis product – hydroxylamine – is also well known as a good reductant for Pu(IV), particularly at low acidities [20, 29, 30]. Stoichiometric equations for HAN and XHA reduction reactions are given in Eqs. (5)–(8), with Eqs. (5) and (7) applying when the reductant (HAN, XHA) is in excess and Eqs. (6) and (8) applying when the oxidant (Pu^{4+}) is in excess (*n.b.* the XHA equations are derived by direct analogy with HAN and accounting for our [12] and Karraker's [25] observations of a 2 : 1 stoichiometry in the Ce(IV) + AHA reduction reaction when cerium is in excess). The presence of an induction period might suggest that HAN is the reductant with reduction starting once HAN reaches a significant level. However, in this case experiments with HAN initially present in solution should have led to an elimination of the induction period. That they did not suggests that Pu(IV) is stabilised by XHA complexation either due to a consequent shift in the redox potential for Pu(IV)/Pu(III) that then thermodynamically prohibits reaction with XHA and/or HAN or because reduction may be kinetically hindered due to steric effects.
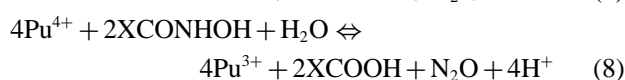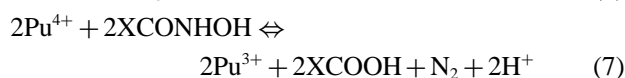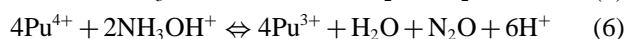
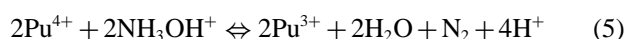$$2Pu^{4+} + 2NH_3OH^+ \Leftrightarrow 2Pu^{3+} + 2H_2O + N_2 + 4H^+ \quad (5)$$

$$4Pu^{4+} + 2NH_3OH^+ \Leftrightarrow 4Pu^{3+} + H_2O + N_2O + 6H^+ \quad (6)$$

$$2Pu^{4+} + 2XCONHOH \Leftrightarrow$$
$$2Pu^{3+} + 2XCOOH + N_2 + 2H^+ \quad (7)$$

$$4Pu^{4+} + 2XCONHOH + H_2O \Leftrightarrow$$
$$4Pu^{3+} + 2XCOOH + N_2O + 4H^+ \quad (8)$$

Table 3. E_f values for solutions of 0.001 M Pu^{4+} in 0.1 M HNO_3 with varying AHA concentrations.

AHA : Pu ratio	0	0.5	1	2	3	4	6	8	10	20
E_f $Pu^{4+/3+}$ (mV Ag/AgCl)	733	731	646	645	625	610	621	603	598	598
E_f $Fe^{3+/2+}$ (mV Ag/AgCl)	400				373	401	440	412		
E_f $Pu^{4+/3+}$ (mV adjusted)[a]	733				652	609	581	591		

a: E_f $Pu^{4+/3+}$ adjusted to correspond with an E_f of 400 mV for $[Fe(CN)_6]^{3-/4-}$.

Cyclic voltammetry was used to investigate the shift in the Pu(IV)/(III) redox couple in the presence of AHA. In an initial trial experiment the cyclic voltammograms (CVs) of a solution containing 0.001 M Pu(IV) in 0.1 M HNO_3 were recorded using a Pt working electrode at scan rates of 50, 100 and 200 mV s^{-1}. Plots of measured peak currents, i_{pa} and i_{pc}, against the square root of the scan rate, $v^{1/2}$ were linear indicating that the electron transfer was close to diffusion controlled. Peak potentials were invariant with v indicating that the reaction was electrochemically reversible under these conditions. The ratios of the peak currents i_{da}/i_{dc} were close to 1, again indicating that the process was chemically and electrochemically reversible at the scan rates used. After correction for internal cell resistance the value of E_f for the $Pu^{4+/3+}$ couple was found to be $+0.733$ V (*vs.* SSCE) or $+0.942$ V (*vs.* NHE). This value lies between the values of $+0.885$ and $+0.966$ V (*vs.* NHE) that we have calculated as the standard electrode potentials for the $Pu(NO_3)_2^{2+}/Pu^{3+}$ and $Pu(NO_3)^{3+}/Pu^{3+}$ systems, respectively (see Fig. 12, *vide infra*). This suggests that the Pu(IV) is present as a mixture of $Pu(NO_3)^{3+}$ and $Pu(NO_3)_2^{2+}$ species under the conditions studied.

Adding 0.1 M AHA solution (AHA : Pu = 6 : 1) and scanning at 50, 100 and 200 mV s^{-1} (Fig. 9) also gave linear plots of i_{pa} and i_{pc} against $v^{1/2}$ with a near zero intercept and current ratios (i_{da}/i_{dc}) close to 1. Peak potentials were again invariant with v, suggesting that the system is behaving reversibly under these conditions. After correction for internal cell resistance the value of E_f was found to be $+0.581$ V (*vs.* SSCE) corresponding to a shift on complexation by acetohydroxamate of 0.152 V from the value of E_f recorded for the $Pu^{4+/3+}$ couple in 0.1 M HNO_3 (Fig. 10). A solution of $K_3[Fe(CN)_6]$ was added and the value of E_f for the $[Fe(CN)_6]^{3-/4-}$ couple under these conditions was found to be $+0.4$ V (*vs.* SSCE).

A series of CVs with 0.001 M Pu^{4+} in 0.1 M HNO_3 but with varying AHA : Pu ratios gave E_f (*vs.* SSCE) values for the $Pu^{IV/III}$ couple given in Table 3. The value obtained for an AHA : Pu ratio of 6 : 1 is *ca.* 40 mV greater than that obtained in the preliminary experiment. However the E_f value for the $[Fe(CN)_6]^{3-/4-}$ couple was also found to be *ca.* 40 mV greater suggesting that the difference is due to a junction potential or other changed feature of the experimental set up used. In some of the solutions the CV wave of the added $[Fe(CN)_6]^{3-}$ did not give clearly defined peak potentials so that a similar adjustment could not be applied. Where the potential of the $[Fe(CN)_6]^{3-/4-}$ couple could be determined, adjusted values for the E_f of the $Pu^{IV/III}$ couple
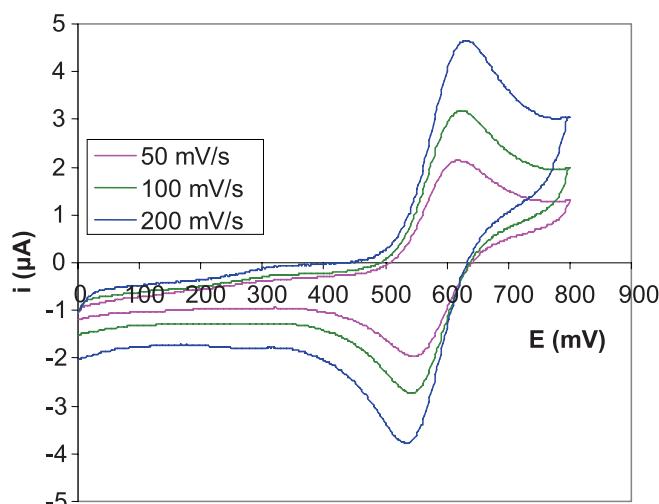
Fig. 9. CVs of a solution containing 0.001 M Pu^{4+} and 0.006 M AHA in 0.1 M HNO_3.
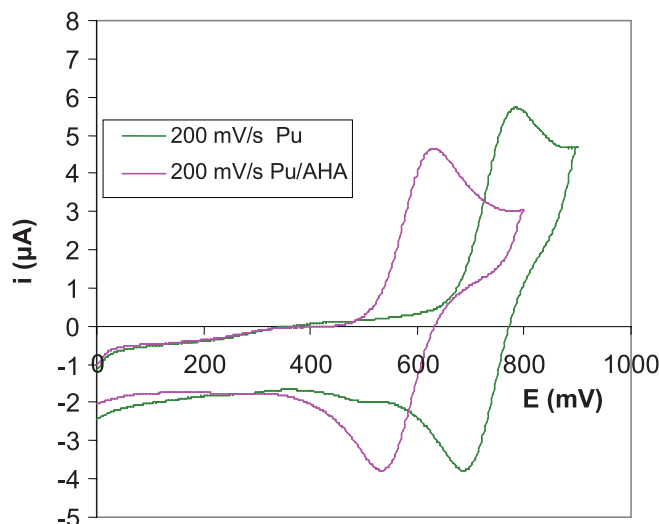
Fig. 10. The shift in potential of the $Pu^{4+/3+}$ couple on the addition of AHA to Pu in a solution of 0.001 M Pu^{4+} in 0.1 M HNO_3 (AHA : Pu = 6 : 1).

are also shown in Table 3. Despite the problems with the accuracy of the potential measurements, the general trend suggests that the potential of the $Pu^{IV/III}$ couple decreases in the presence of AHA to reach an essentially constant value when, or just before, the AHA : Pu ratio reaches 6 : 1. This agreed with the EAS of 0.001 M Pu-AHA solutions which showed absorbance at 441 nm (Pu^{IV}-AHA complex peak) reaching a plateau at ∼ 6 : 1 AHA : Pu ratio (in 1 M HNO_3).

Table 4. The variation in E_f with acidity for solutions containing 0.001 M Pu^{4+} and 0.01 M AHA.

Acidity	0.1	0.5	1.0	1.5	2.0	2.5	3.0
E_f (mV)[a]	600	627	646	656	652	656	646

a: The E_f values (*vs*. Ag/AgCl) quoted here were not corrected for *iR* drop and this is expected to result in a high bias of between 1 and 5 mV in the values cited.
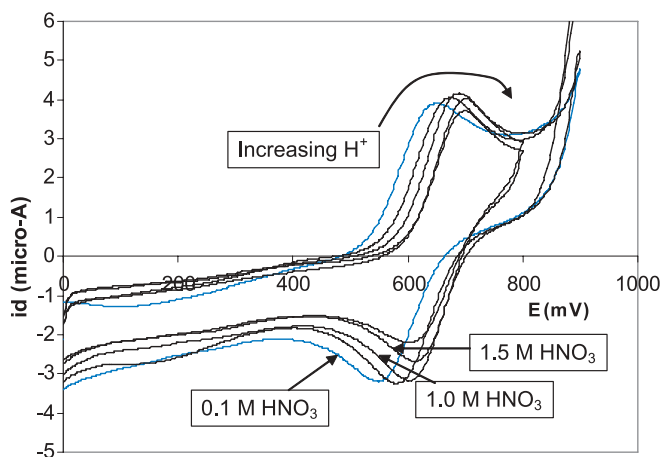

Fig. 11. Selected CVs of solutions containing 0.001 M Pu(IV) and 0.01 M AHA at varying acidities. Lines correspond to CVs at 0.1, 0.5, 1.0, 1.5 and 3 M HNO_3 (data at 2.0 and 2.5 M HNO_3 not included).

In order to assess the effect of acidity on the potential of the $Pu^{IV/III}$ couple in the presence of AHA a series of measurements was made on solutions containing 0.001 M Pu^{4+} and 0.01 M AHA in various concentrations of acid. Representative examples of the CVs obtained are shown in Fig. 11 and the numerical results in Table 4. Between 0.1 and 1.5 M HNO_3 there is a shift in the formal potential of the $Pu^{IV/III}$ couple with increasing acidity towards the value found in the absence of AHA (*i.e.* $+0.733$ V *vs*. SSCE). This reflects decomplexation/speciation changes and correlates with the EAS which start to show the presence of small amounts of $Pu(NO_3)^{3+}$ (peak at ~ 476 nm) from an acidity of 1.5 M HNO_3 upwards. Between 1.5 and 3 M HNO_3 there is no consistent change in potential, the values all being in the range 651 ± 5 mV.

3.3.2 Discussion

Preliminary speciation diagram calculations indicate that, at 0.008 M total AHA, Pu(IV) exists predominantly as the 1 : 1 Pu : AHA complex at 1 M HNO_3 [28]. In the same system at 0.1 M HNO_3, Pu(IV) exists as a mix of the 1 : 1 and 1 : 2 Pu : AHA complexes with the 1 : 1 complex being approximately twice the concentration of the 1 : 2 complex [28]. By use of those equilibrium constants for formation of the 1 : 1 and 1 : 2 Pu(IV) : AHA species in nitric acid derived from stability constant measurements in $HClO_4$ [12] and Pu(IV) nitrate complexation constants [31], it is possible through use of Eq. (9) and the standard electrode potential for the $Pu^{4+/3+}$ couple [32], to calculate the standard electrode potentials for the $Pu(AHA)^{3+}/Pu^{3+}$ and $Pu(AHA)_2{}^{2+}/Pu^{3+}$ couples:

$$E^\theta_{Pu(AHA)^{3+}/Pu^{3+}} = E^\theta_{Pu^{4+}/Pu^{3+}} - \frac{RT}{F} \ln K_1 \tag{9a}$$

$$E^\theta_{Pu(AHA)_2{}^{2+}/Pu^{3+}} = E^\theta_{Pu(AHA)^{3+}/Pu^{3+}} - \frac{RT}{F} \ln K_2$$

$$= E^\theta_{Pu^{4+}/Pu^{3+}} - \frac{RT}{F} \ln K_1 K_2 , \tag{9b}$$

where K_1 and K_2 are the equilibrium constants for the following systems:

$$AHA + Pu^{4+} \xleftarrow{K_1} Pu(AHA)^{3+} + H^+ \tag{10a}$$

$$AHA + Pu(AHA)^{3+} \xleftarrow{K_2} Pu(AHA)_2{}^{2+} + H^+ . \tag{10b}$$
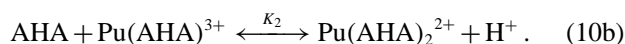
This assumes that the complexes are labile and rapid ligand dissociation accompanies reduction. The apparently reversible character of the cyclic voltammograms obtained in the absence of AHA and at AHA : Pu ratios above 5 : 1 suggest that the ligand dissociation reactions are rapid on the cyclic voltammetry timescales studied here and do indeed involve highly labile species. From these calculated standard potentials it is possible to estimate the formal potential, E_f, of the $Pu(AHA)^{3+}/Pu^{3+}$ and $Pu(AHA)_2{}^{2+}/Pu^{3+}$ redox couples by writing the Nernst equation for each couple (incorporating the standard electrode potentials as determined by Eq. (11) and setting $[Pu^{4+}]$, $[Pu(AHA)^{3+}]$ and $[Pu(AHA)_2{}^{2+}]$ therein equal to 1 M). This gives:

$$E_\mathrm{f}\left(Pu(AHA)^{3+}/Pu^{3+}\right) =$$
$$E^\theta_{Pu(AHA)^{3+}/Pu^{3+}} + \frac{RT}{F} \ln\left(\frac{[H^+]}{[AHA]}\right) \tag{11a}$$

$$E_\mathrm{f}\left(Pu(AHA)_2{}^{2+}/Pu^{3+}\right) =$$
$$E^\theta_{Pu(AHA)_2{}^{2+}/Pu^{3+}} + \frac{RT}{F} \ln\left(\frac{[H^+]^2}{[AHA]^2}\right) , \tag{11b}$$

from which can be calculated values of $+0.808$ V and $+0.867$ V (*vs*. NHE) for the reduction of the 1 : 1 complex in 0.008 M total AHA solutions at 0.1 and 1 M HNO_3, respectively; and calculated values of $+0.825$ and $+0.943$ V (*vs*. NHE) for the reduction of the 2 : 1 complex in 0.008 M total AHA solutions at 0.1 and 1 M HNO_3, respectively.

The measured and calculated formal potentials for the $Pu^{4+}/HNO_3/AHA$ system are summarized in Fig. 12. Electrochemical measurements on nitric acid solutions of Pu^{4+} containing the complexing agent AHA (Table 3) show that the presence of AHA has a stabilising effect on Pu^{4+} with respect to reduction, this resulting from the complexation of Pu^{4+} with hydroxamate. The measured shift in the $Pu^{IV/III}$ potential in 0.1 M and 1 M HNO_3 when AHA was added in an AHA : Pu ratio of 8 : 1 were 141 and 49 mV, respectively.

Fig. 12 also shows that, within experimental error, the measured formal potential of the 8 : 1 AHA : Pu solution ($+0.858$ V *vs*. NHE) in 1 M nitric acid is barely distinguishable from the onset potential of $+0.861$ V (*vs*. NHE) reported for AHA oxidation [19], although it should be noted that the latter was obtained at a gold electrode [33], which is not chemically inert under these conditions. Therefore, the potential data summarised in Fig. 12 suggest that AHA itself should reduce free Pu^{4+} to Pu^{3+} but cannot reduce either the 1 : 1 or 2 : 1 AHA Pu complexes.

Measured Values   **Calculated Values**

Potential (V) vs NHE

$E^0_{Pu^{4+}/Pu^{3+}} = +1.01$

+0.941 Pu^{4+}/Pu^{3+}, 0.1M HNO$_3$

+0.920 Pu^{4+}/Pu^{3+}, 1M HNO$_3$

+0.907 Pu^{4+}/Pu^{3+}, 1M HNO$_3$

+0.861 AHA Oxidation onset

+0.858 8:1 AHA:Pu^{4+}, 1M HNO$_3$

+0.800 8:1 AHA:Pu^{4+}, 1M HNO$_3$

+0.966 [Pu(NO$_3$)]$^{3+}$/ Pu^{3+}

+0.885 [Pu(NO$_3$)$_2$]$^{2+}$/ Pu^{3+}

+0.867 PuAHA^{3+}/Pu^{3+}, 1M HNO$_3$

+0.825 Pu(AHA)$_2$$^{2+}$/Pu^{3+}

+0.816 [Pu(NO$_3$)$_3$]$^{+}$/ Pu^{3+}

+0.808 PuAHA^{3+}/Pu^{3+}, 0.1M HNO$_3$

+0.511 [Fe(CN)$_6$]$^{3-/2-}$, 1M HClO$_4$

+0.509 [Fe(CN)$_6$]$^{3-/2-}$, 1M HNO$_3$

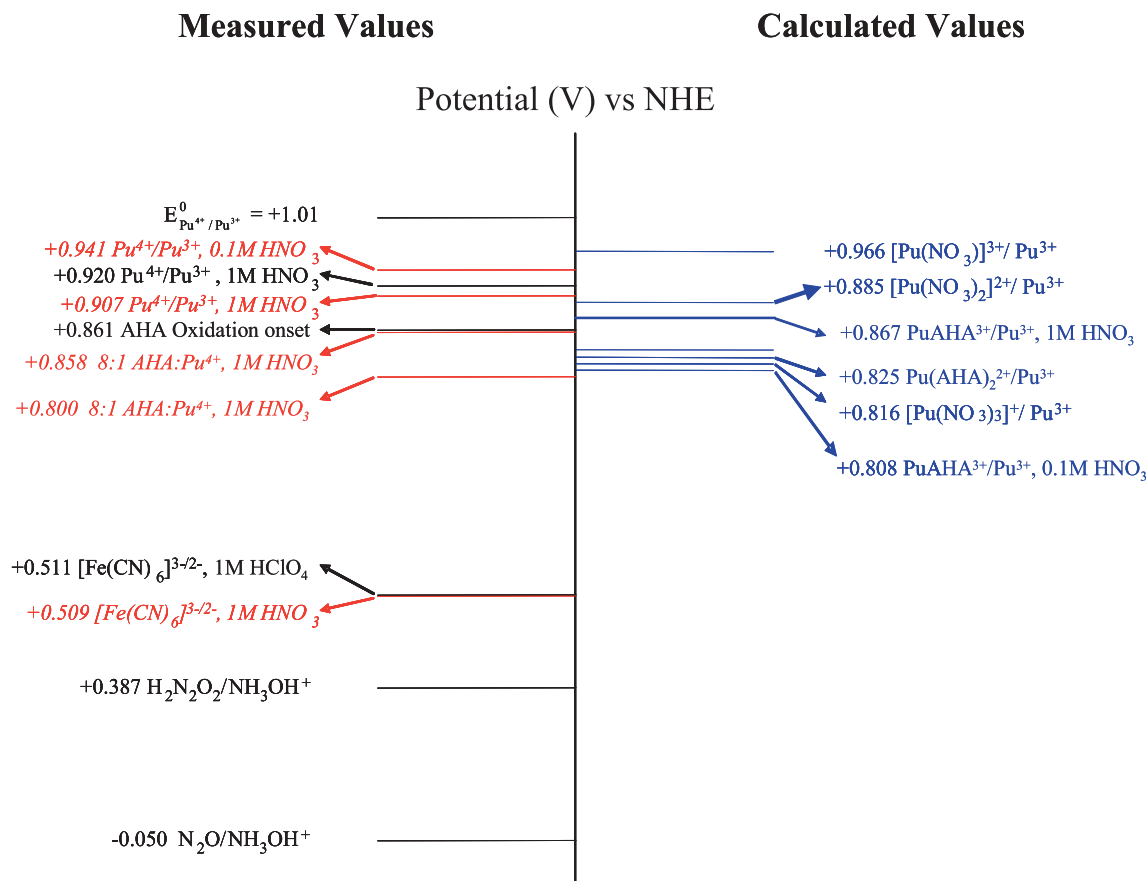+0.387 H$_2$N$_2$O$_2$/NH$_3$OH$^+$

-0.050 N$_2$O/NH$_3$OH$^+$

Fig. 12. Schematic potential diagram showing the measured (measured numbers in italic are extracted from this work, those in normal font are from published data) and calculated formal potentials for the Pu^{4+}/HNO$_3$/AHA system.

Comparison of the experimentally determined formal potentials for the 8 : 1 AHA : Pu systems at 0.1 and 1 M HNO$_3$ with the calculated formal potential values for those systems (*vide supra* and the right hand side of Fig. 12) indicates that the experimentally determined values most closely correspond with the calculated values for the 1 : 1 complex at both nitric acid concentrations. This is in agreement with the preliminary speciation data cited at the beginning of this section.

Thermodynamically, hydroxylamine should reduce Pu(IV)-AHA complexes so the fact that it does not appear to do so in our experiments implies some kinetic hindrance perhaps due to steric constraints. The reductant for Pu(IV) ions in this Pu(IV)/AHA/HNO$_3$ system therefore seems most likely to be the AHA. Whether this is a reaction between de-complexed Pu^{4+}(aq) and solution phase AHA or whether it may be as a result of 'internal' electron transfer as a bound hydroxamate ligand hydrolyses *in-situ* is currently only speculation.

4. Conclusion

It is well known that simple hydroxamic acids such as FHA and AHA are unstable in acid solution undergoing acid hydrolysis to form the parent carboxylic acid and hydroxylamine. We have determined the kinetic rate equations for these reactions, including activation energies and nitrate dependencies. These are consistent with the general literature on hydroxamic acid hydrolysis. Pu(IV) forms strong complexes with these hydroxamate ligands even in acid solutions but these complexes are unstable with Pu(III) eventually being formed in solution. The reductions of Pu(IV) in the presence of FHA and AHA have been examined. They are consistent with a mechanism in which free hydroxamic acid in solution is hydrolysed whilst Pu(IV) ions remain fully complexed to hydroxamate ligands; then at some point close to a 1 : 1 Pu(IV) : XHA ratio, some free Pu^{4+} is released from the complex and reduction is initiated. Electrochemical and kinetic data suggest that the reductant is the hydroxamic acid rather than the hydroxylamine.

References

1. Chatterjee, B.: Donor properties of hydroxamic acids. Coord. Chem. Rev. **26**, 281 (1978).
2. Raymond, K. N., Freeman, G. E., Kappel, M. J.: Actinide specific complexing agents: their structural and solution chemistry. Inorg. Chim. Acta **94**, 193 (1984).
3. Anderegg, G., L'Eplattenier, F., Schwarzenbach, G.: Hydroxamatkomplexe II. Die Anwendung der pH-Methode. Helvet. Chim. Acta **46**, 1400 (1963).
4. Barocas, A., Baroncelli, F., Biondi, G. B., Grossi, G.: The complexing power of hydroxamic acids and its effect on behaviour of organic extractants in the reprocessing of irradiated fuels-II. J. Inorg. Nucl. Chem. **28**, 2961 (1966).

5. Baroncelli, F., Grossi, G.: The complexing power of hydroxamic acids and its effect on behaviour of organic extractants in the reprocessing of irradiated fuels-I. J. Inorg. Nucl. Chem. **27**, 1085 (1965).

6. Colston, B. J., Choppin, G. R., Taylor, R. J.: A preliminary study of the reduction of Np(VI) by formohydroxamic acid using stopped-flow near-infrared spectrophotometry. Radiochim. Acta **88**, 329 (2000).

7. Chung, D. Y., Lee, E. H.: The reduction of Np(VI) by acetohydroxamic acid in nitric acid solution. In: *Recent Advances in Actinide Science*. (Alvarez, R., Bryan, N. D., May, I., eds.) Royal Society of Chemistry, Cambridge (2006), pp. 587–589.

8. Fox, O. D., Jones, C. J., Birkett, J. E., Carrott, M. J., Maher, C. J., Roube, C. V., Taylor, R. J:. Advanced PUREX flowsheets for future Np and Pu fuel cycle demands. In: Separations for the Nuclear Fuel Cycle in the 21st Century. (Lumetta, G. J., Nash, K. L., Clark, S. B., Friese, J. I., eds.) ACS Symposium Series 933, American Chemical Society, Washington DC (2006), pp. 89–102.

9. Birkett, J. E., Carrott, M. J., Fox, O. D., Jones, C. J., Maher, C. J., Roube, C. V., Taylor, R. J., Woodhead, D. A.: Controlling neptunium and plutonium within single cycle solvent extraction flowsheets for advanced fuel cycles. J. Nucl. Sci. Technol. **44**, 337 (2007).

10. Zilberman, B. Ya., Fedorov, Yu. S., Mishin, E. N., Sytnik, L. V., Shmidt, O. V., Kukharev, D. N., Goletsky, N. D., Glekov, R. G., Palenik, Yu. V., Sukhareva, S. Yu.: Superpurex as a TBP-compatible process for recovery and partitioning of long lived radionuclides from NPP spent fuel. In: Proceedings of the International Symposium NUCEF 2001 – Scientific Basis for Criticality Safety, Separation Process and Waste Disposal. (Banba, T., Tsubata, Y., eds.) JAERI-Conf 2002-004, Tokai-Mura (2002), pp. 189–196.

11. Todd, T. A., Wigelund, R. A.: Advanced separation technologies for processing spent nuclear fuel and the potential benefits to a geologic repository. In: Separations for the Nuclear Fuel Cycle in the 21st Century. (Lumetta, G. J., Nash, K. L., Clark, S. B., Friese, J. I., eds.) ACS Symposium Series 933, American Chemical Society, Washington DC (2006), pp. 41–56.

12. Carrott, M. J., Fox, O. D., Maher, C. J., Mason, C., Taylor, R. J., Sinkov, S., Choppin, G. R.: Solvent extraction behaviour of plutonium(IV) ions in the presence of simple hydroxamic acids. Solv. Extr. Ion. Exch. **25**, 723 (2007).

13. Miles, J. H., Temple, W.: An analytical method and hydrolysis data for a new U/Pu separating reagent. Unpublished report, AEA-FS-0178(H), Harwell (1993).

14. Mane, B. S., Jagdale, M. H.: Kinetics of the acid catalysed hydrolysis of isobutyrohydroxamic acid. J. Ind. Chem. Soc. **LIV**, 615 (1977).

15. Taylor, R. J., Boxall, C., Andrieux, F., Mason, C.: Modelling the hydrolysis of actinide complexed hydroxamic acid ligands. In: *Recent Advances in Actinide Science*. (Alvarez, R., Bryan, N. D.,

May, I., eds.) Royal Society of Chemistry, Cambridge (2006), pp. 626–628.

16. Laidler, K. J., Meiser, J. H.: *Physical Chemistry*. The Benjamin/Cummings Publishing Company Inc., California (1982).

17. Cohen, D. J.: The absorption spectra of plutonium ions in perchloric acid solutions. Inorg. Nucl. Chem. **18**, 211 (1961).

18. May, I., Taylor, R. J., Denniss, I. S., Wallwork, A. L., May, I.: Czech J. Phys. **49**, 597 (1999).

19. Taylor, R. J., May, I.: The reduction of actinide ions by hydroxamic acids. Czech J. Phys. **49**, 617 (1999).

20. Barney, G. S.: A kinetic study of the reaction of plutonium(IV) with hydroxylamine. J. Inorg. Nucl. Chem. **38**, 1677 (1976).

21. Bard, A. J., Parsons, R., Jordon, J.: *Standard Potentials in Aqueous Solution*. Marcel Dekker, New York (1985).

22. Ghosh, K. K.: Kinetic and mechanistic aspects of acid-catalysed hydrolysis of hydroxamic acids. Ind. J. Chem. **36B**, 1089 (1997).

23. Mane, B. S., Jagdale, M. H.: Kinetics of the acid catalysed hydrolysis of hexanohydroxamic acid. Ind. J. Chem. **15A**, 1086 (1977).

24. Mane, B. S., Jagdale, M. H.: Kinetics of the acid catalyzed hydrolysis of hydroxamic acids. React. Kinet. Catal. Lett. **6**, 417 (1977).

25. Karraker, D. G., Rudisill, T. S., Thompson, M. C.: Studies of the effect of acetohydroxamic acid on plutonium and neptunium by 30 vol. % tributyl phosphate. WSRC-TR-2001-00509, Westinghouse Savannah River Company, http://www.osti.gov/bridge/.

26. Miles, J. H.: Separation of plutonium and uranium. In: *Science and Technology of Tributyl Phosphate, Volume III*. (Schulz, W. W., Burger, L. L., Navratil, J. D., eds.) CRC Press Inc., Boca Raton (1990), pp. 11–54.

27. Taylor, R. J., Mason, C., Cooke, R., Boxall, C.: The reduction of Pu(IV) by formohydroxamic acid in nitric acid. J. Nucl. Sci. Technol. Suppl. **3**, 278 (2002).

28. Andrieux, F. P. L., Boxall, C., Taylor, R. J.: The hydrolysis kinetics of hydroxamic acid complexants in the presence of oxidising plutonium(IV). Inorg. Chem., under review (2008).

29. Koltunov, V. S., Zhuravleva, G. I.: Kinetics of actinide reduction by hydroxylamine. III. Plutonium(IV) reduction in nitric acid solution. Radiokhim. **20**, 94 (1978).

30. Koltunov, V. S., Zhuravleva, G. I.: Kinetics of actinide reduction by hydroxylamine. IV. Plutonium(IV) reduction in perchloric acid solution. Radiokhim. **20**, 661 (1978).

31. Clark, D. L., Hecker, S. S., Jarvinen, G. D., Neu, M. P.: Plutonium. In: *The Chemistry of the Actinide and Transactinide Elements*. (Morss, L. R., Edelstein, N. M., Fuger, J. R., eds.) 3rd Edn., Springer, Dordrecht (2006), pp. 813–1265.

32. Bard, A. J., Faulkner, J. R.: *Electrochemical Methods Fundamentals and Applications*. J. Wiley & Sons, New York (1980).

33. Shackleford, S.: Development of an EQCM-based sensor for metal ions. Ph.D. Thesis, University of Central Lancashire, Preston (2002).